

SUPERCONDUCTIVITY IN HIGH FREQUENCY FIELDS

I.O.Kulik

Department of Physics, Bilkent University, Ankara, Turkey

Abstract- Fundamentals of BCS and GLAG theories of superconductivity are reviewed with a focus on high-frequency properties of bulk superconductors, superconducting films and superconducting cavities. Superconductivity as a macroscopic quantum coherent state. Supercurrents and persistent currents. Condensate and excitations. Complex penetration depth and RF losses. Mechanisms of Q degradation in superconducting cavities. Depairing effects and vortex nucleation mechanisms. Surface superconductivity and tilted vortices. Material parameters and factors responsible for ultimate performance of superconducting resonators.

Superconductivity bears its applications owing to zero d.c. resistance and extremely small a.c. losses, magnetic flux expulsion (the Meissner effect) and the possibility of generating very high magnetic fields, flux quantization and extreme sensitivity of weak coupled superconductors (Josephson junctions) to small electromagnetic fields. The first decisive measurement of zero resistance in superconductor was done by G.Holst [1] in Kamerlingh Onnes Laboratory [2]. A variety of superconducting materials with critical temperature in the range 1-23 K have been found following the seminal work of Kamerlingh Onnes and, at latest time, resulted in the discovery of superconducting materials with a critical temperature above 100 K [3,4].

Superconductivity belongs to one of most remarkable phenomena in condensed matter physics, and in physics in general. It starts with specific kind of macroscopic ordering similar, and at the same time extending, the another types of macroscopic order: crystals (Fig.1,a), ferromagnets (Fig.1,b). In

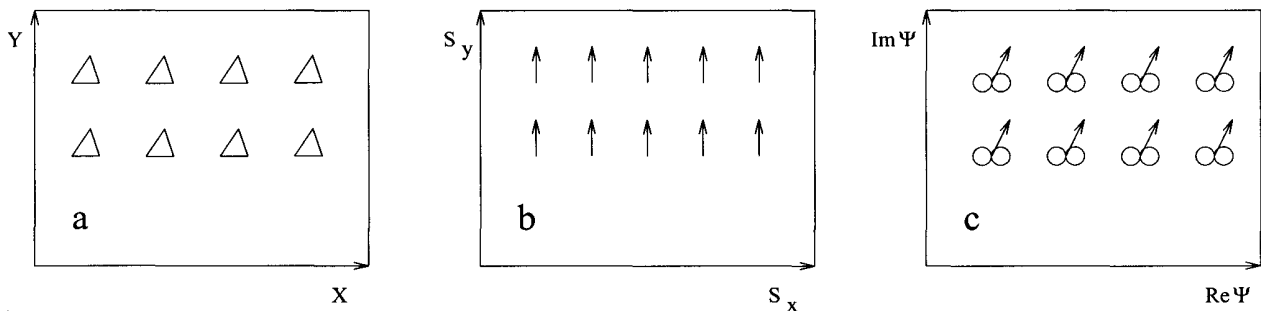


Fig.1 Macroscopic order in crystals (a), ferromagnets (b) and superconductors (c).

superconductor, in contrast to those classically describable types of long range order, **phases** of the wave functions of electronic pairs become correlated at macroscopic distances providing for macroscopic order in the $(\text{Re } \Psi, \text{Im } \Psi)$ space (Fig.1,c). All mentioned types of ordering are of quantum nature. Crystalline order is generally not considered as a wonder (which it is), and similarly magnetic ordering of spins in ferromagnetic solids is readily accepted. Superconducting order is harder to comprehend since it relates to a nonclassical entity, Ψ . It lasted almost 50 years from the discovery until superconductivity was properly understood in the theory developed by Bardeen, Cooper and Schrieffer [5] (the “BCS model”). Behavior of superconductors in the electromagnetic field is adequately described within the GLAG (Ginzburg-Landau-Abrikosov-Gorkov) theory [6-8]. Basic properties of superconductors are accounted for within the BCS-GLAG scheme and are listed schematically in Fig.2. Table I includes characteristic representatives of various classes of superconducting materials and their critical parameters - critical magnetic field H_c and critical temperature T_c .

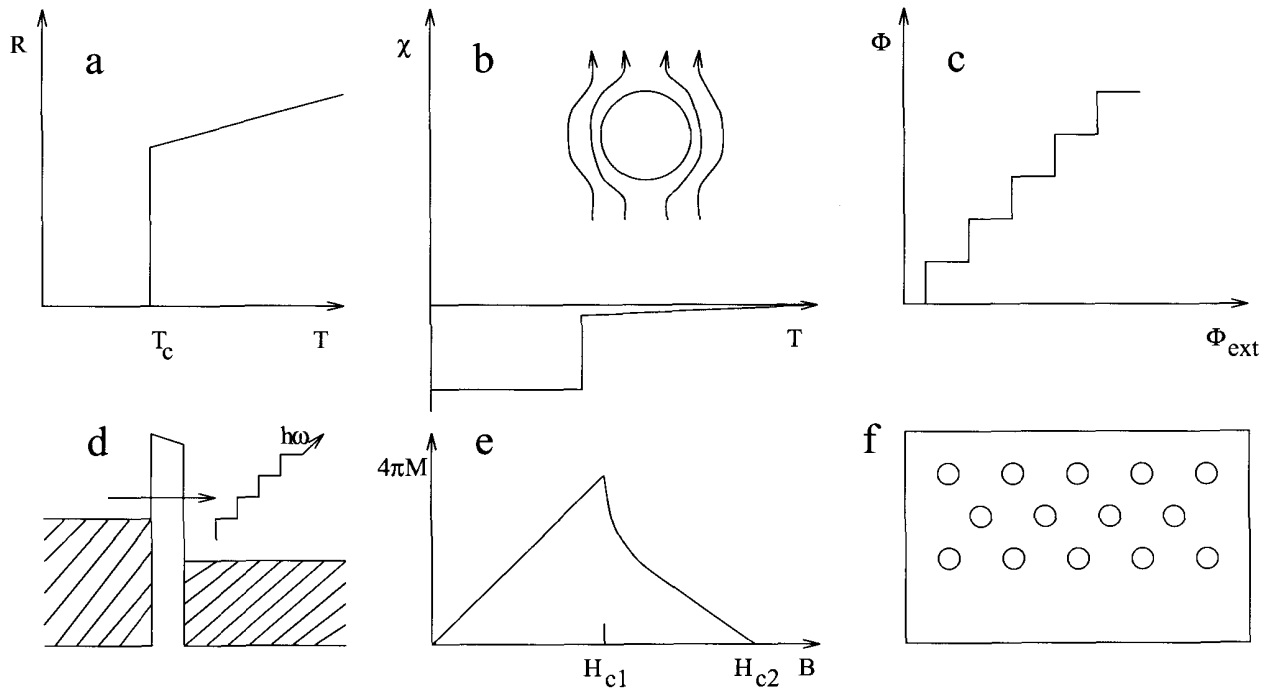


Fig.2. Basic properties of superconductors. (a) Zero resistance , (b) Meissner effect, (c) flux quantization, (d) Josephson effect, (e,f) mixed state and Abrikosov vortices.

Table 1. Basic parameters of superconducting materials

Superconductor	T_c, K	H_c, T	Structure / type / nickname
<i>Nb</i>	9.3	0.2	Elemental superconductors
<i>Nb₃Ge</i>	23	38	Intermetallics
<i>Nb – Ti</i>	10	10	Alloys
<i>Ba_{1-x}K_xBiO₃</i>	30		Perovskites
<i>Sn_xMo₆S₈</i>	14	50	Chevrel phases
<i>CeCu₂Si₂</i>	0.6	2.4	Heavy fermions
<i>ErRh₄B₄</i>	8.7		Magnetic superconductors
<i>LuNi₂B₂C</i>	16		Borocarbides
<i>PdH(Cu, Ag, Au)</i>	17		Palladium-hydrogen
<i>BEDT – TTF</i>	14		Organic superconductors
<i>La_{2-x}Sr_xCuO₄</i>	35		Oxides
<i>YBa₂Cu₃O₇</i>	95	200	YBCO
<i>Bi₂Sr₂Ca₂Cu₃O₁₀</i>	110		BISCO
<i>Tl₂Ba₂Ca₂Cu₃O₁₀</i>	125		Thallium-compound
<i>HgBa₂Ca₂Cu₃O₈</i>	133		Mercury-compound
<i>Cs_xC₆₀</i>	43	20	Fullerenes

Origin of superconductivity relates to the interaction between electrons and quantized vibrations of crystalline lattice, the phonons. In the ground state of a metal, electrons from the outer atomic shells delocalize to form a “Fermi liquid”, a state in which all electrons are confined within the “Fermi sphere” located in the momentum space at the center of the Brillouin zone (Fig.3,a). Phonons occupy all states within the full Brillouin zone (Fig.3,b). These are virtual particles which do not contribute to thermal part of free energy and are not detected in an experiment. However, such virtual states are important for superconductivity.

Thermal excitations are electrons near the Fermi energy (Fig.3,c) and phonons near the origin of the momentum space (Fig.3,d). Properties of metal in the normal state relate to these excitations. In superconductor, virtual phonons produce an attractive interaction between electrons which appears due to deformation of phonon continuum by an electron. Another electron experiences drag due to continuum deformation. Virtual phonons serve as mediators of electron-electron attraction which results in formation of bound electron pairs near the Fermi surface. The pairs are Bose-particles which condense in the momentum space as described above. The unpaired electrons remain as “quasiparticles” responsible for dissipation at the non-zero frequency.

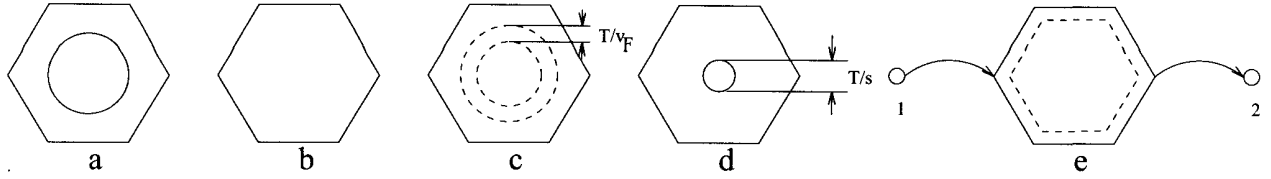


Fig.3. (a) Electronic “vacuum” (electrons inside the Fermi sphere) and (b) “vacuum” of phonons (the virtual phonons). States between dashed lines in (c) represent electronic excitations, states near the origin in (d) - phononic excitations (thermal phonons). Interaction between electrons 1 and 2 is mediated by the phonon vacuum deformation (e).

The concentration of quasiparticles increases with increase of temperature while concentration of paired electrons goes down. At certain temperature T_C superconductivity is destroyed. There are two types of electronic excitations, those with momentum smaller than the Fermi momentum p_F (quasi-electrons) and excitations with $p < p_F$ (quasi-holes). Energy of quasiparticle of either type is given by

$$\varepsilon_p = \sqrt{\Delta^2 + \xi_p^2}, \quad \xi_p = v_F |p - p_F| \quad (1)$$

where Δ is an energy gap [5]. Creating an excited state over the electron “vacuum” can be achieved by either removing an electron from the Fermi surface and placing it above the surface, or by removing an electron from below the Fermi surface and placing it at the surface. At superconducting transition, electron vacuum of a normal metal transforms to the condensate of electron pairs (the Cooper pairs). Nontrivial circumstance is that the condensate, or restructured electron vacuum, can support an electric current if displaced in a momentum space by some vector \vec{p}_s : $\vec{j}_s = n_s e \vec{v}_s$ where $\vec{v}_s = \vec{p}_s / 2m$. n_s is called the “superelectron concentration” (twice the concentration of Cooper pairs). At increasing temperature, concentration of quasiparticles increases and n_s decreases.

Below T_C , both condensate and excitations coexist and current may have a component proportional to the electric field

$$\vec{j} = \vec{j}_s + \vec{j}_n, \quad \vec{j}_n = \sigma \vec{E} = -(\sigma / c) \partial \vec{A} / \partial t, \quad \vec{j}_s = n e \vec{v}_s \quad (3)$$

and

$$\vec{v}_s = \frac{1}{2m} \left(\vec{p}_s - \frac{2e}{c} \vec{A} \right). \quad (4)$$

Expression (4) explains the phenomenon of flux quantization in the hollow superconducting cylinder: since the azimuthal momentum of the pair is quantized

$$p_\varphi = nh / L, \quad n = 0, \pm 1, \pm 2, \dots \quad (5)$$

where L is the circumference of the cylinder cross section, and \vec{v}_s vanishes inside superconductor due to the Meissner effect, the magnetic flux $\Phi = \oint \vec{A} d\vec{l} = \int \vec{H} d\vec{S}$ becomes multiple of Φ_0 . The minimal amount of flux between successive values of n is called “flux quantum” $\Phi_0 = hc / 2e = 2 \cdot 10^{-7} G \cdot cm^2$. After switching off the magnetic field, the flux $\Phi = n\Phi_0$ may be trapped inside the cylinder.

In a thin-walled superconducting cylinder, an external vector-potential $A = A_\phi$ will induce a current which quadratically increases with A at small A (Fig.4). Energy increases quadratically with A . There exists an infinite number of states with energies $E_n(A)$ for various values of n .

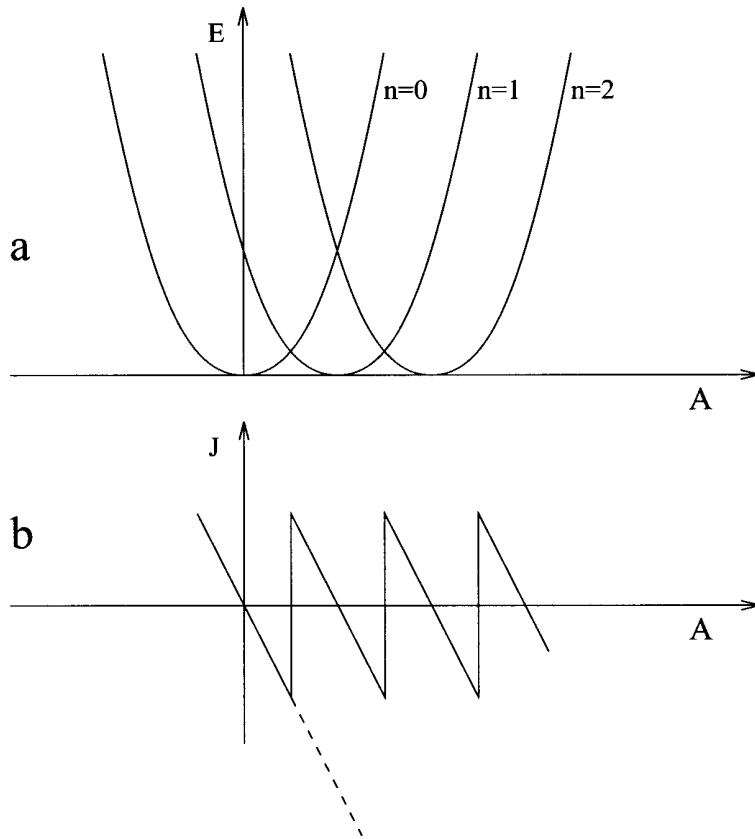


Fig.4. Energy vs vector potential (a) and current vs vector potential (b) dependences in a hollow superconducting cylinder. Solid line in (b) corresponds to the persistent current in the cylinder wall, dashed line to a supercurrent.

Switching between these states to assume a minimal energy at given value of A , would require “macroscopic excitation”, a transition in a physical vacuum requiring that macroscopic (and therefore very large -of order 10^{23} per cubic centimeter) number of Cooper pairs transits coherently. Such excitations are topological in the wave-function parameter space and require minimal energy of order $\frac{H_c^2}{8\pi} \xi^3$ where ξ is the coherence length of superconductor. At $T = 0$, coherence length equals

$$\xi_0 = \frac{\hbar v_F}{2\pi^2 \Delta(0)} \cong 0.1 - 1 \mu m. \quad (6)$$

Abrikosov vortices [7] are examples of such topological excitations in superconductor. Penetration of the vortex to the superconductor, and its subsequent transformation to the magnetic flux lines inside the cylinder orifice when vortex leaves the cylinder wall, changes the flux by an amount Φ_0 . Starting from a state of the cylinder (Φ, I) and applying external magnetic field, will create a current in the cylinder wall proportional to A . At the value of A corresponding to the intersection between two near parabolas in Fig.4,a, the system may switch between states n and $n \pm 1$ to decrease its energy. If such transition does occur, the current as a function of A would follow the solid line in Fig.4,a. If, on the other hand, the value of n is fixed, current will increase further as depicted by a dashed line. The critical value of A corresponding to the intersection of parabolas is extremely small since it is inversely proportional to macroscopic parameter, a length of the ring. In a superconducting ring or cylinder exposed to vector potential, current passes very many times through the intersections, not switching to the lower-energy states.

In case of a steady current, the full line in Fig.4,b is said to correspond to **persistent current** whereas the dashed line to **supercurrent**. Persistent current is an equilibrium property. Such currents never decay since there is no way of reaching lower energy at any given value of A . Similar currents, but however of much smaller amplitude, exist in the non-superconducting (normal) mesoscopic rings and cylinders [10,11].

Supercurrent, unlike the persistent current, is in principle a finite-lived phenomenon in a metastable rather than true stable state. However, the relaxation time of such metastable state is astronomically large for any reasonable size of superconducting device, e.g., superconducting cavity. In the case of a.c. currents in cavities, much more important source of dissipation comes from the quasiparticle rather than condensate relaxation.

The total current in an external time-dependent electric field $E = E_\omega e^{-i\omega t}$ is expressed according to Eq.(3) as

$$j_\omega = \sigma(\omega)E_\omega, \quad \sigma = \sigma_1(\omega) + i\sigma_2(\omega) \quad (7)$$

where σ_1 is related to supercurrent, σ_2 to normal current. The theory of frequency and wave-vector dependent linear response of superconductor to the electromagnetic field was developed by Abrikosov, Gorkov and Khalatnikov [13] and by Mattis and Bardeen [14]. In the local limit corresponding to the small value of the coherence length ξ_0 compared to k^{-1} , electrodynamics of superconducting state can be adequately described by the concept of the "complex penetration depth" $\delta(\omega)$ such that

$$\frac{1}{\delta^2} = \frac{1}{\delta_L^2} - \frac{2i}{\delta_{sk}^2} \quad (8)$$

where

$$\delta_L = (mc^2 / 4\pi n_s e^2)^{1/2}, \quad \delta_{sk} = (c^2 / 2\pi\sigma_2 \omega)^{1/2} \quad (9)$$

are the London penetration depth and the skin penetration depth, respectively.

In the extreme local limit, $\delta_L \ll \xi_0$ and $l \ll \xi_0$ where l is the mean free path of electron in the normal state, σ_1, σ_2 are frequency dependent. In the frequency domain $h\nu < 2\Delta$ we have

$$\frac{\sigma_1}{\sigma_n} = \frac{1}{\omega} \int_{\Delta}^{\infty} \frac{\varepsilon^2 + \Delta^2 + \omega\varepsilon}{\sqrt{\varepsilon^2 - \Delta^2} \sqrt{(\varepsilon + \omega)^2 - \Delta^2}} \left(\tanh \frac{\varepsilon + \omega}{2T} - \tanh \frac{\varepsilon}{2T} \right) d\varepsilon, \quad (10)$$

$$\frac{\sigma_2}{\sigma_n} = \frac{1}{\omega} \int_{\Delta - \omega}^{\Delta} \frac{\varepsilon^2 + \Delta^2 + \omega\varepsilon}{\sqrt{\Delta^2 - \varepsilon^2} \sqrt{(\varepsilon + \omega)^2 - \Delta^2}} \tanh \frac{\varepsilon + \omega}{2T} \cdot d\varepsilon \quad (11)$$

σ_n is the Drude conductivity of metal in the normal state, $\sigma_n = ne^2 l / p_F$. In case of superconducting cavity, typical relation between Δ, ω and T is such that

$$\omega \ll T \ll \Delta$$

which simplify Eqs.(10),(11) to

$$\frac{\sigma_1}{\sigma_n} \cong \frac{2\Delta}{T} \exp\left(-\frac{\Delta}{T}\right) \ln \frac{9T}{4\omega}, \quad \frac{\sigma_2}{\sigma_n} \cong \frac{\pi\Delta}{\omega}. \quad (12)$$

The value of σ_2 corresponds to the effective superelectron concentration of a dirty metal $n_s = nl / \xi_0$. The imaginary part of conductivity, σ_2 , can be presented in a Drude-like form corresponding to normal electron concentration (quasiparticle concentration)

$$n_{qp} \approx n \frac{\Delta}{T} \exp(-\Delta / T). \quad (13)$$

For simplicity, we neglected the logarithmic frequency dependence of σ_2 . The most important property incipient in Eq.(13) is the exponential dependence of n_{qp} on temperature. This strongly suppresses a.c. losses at temperature $T \ll T_C$.

Electrodynamics of bulk superconducting metals and superconducting films can be described with the introduction of surface impedance Z (in case of bulk superconductor) and matrix of impedances Z_{ik} (in case of superconducting plate of thickness d). The elements of that matrix relate tangential components of magnetic and electric fields at two surfaces [15]

$$\vec{E}_t^- = \zeta_1 \vec{H}_t^- \times \vec{n} - \zeta_2 \vec{H}_t^+ \times \vec{n}, \quad (14a)$$

$$\vec{E}_t^+ = \zeta_2 \vec{H}_t^- \times \vec{n} - \zeta_1 \vec{H}_t^+ \times \vec{n} \quad (14b)$$

where \vec{n} is a unit vector normal to surface and $\zeta_i = Z / Z_0$, $Z_0 = 4\pi / c$ is the impedance of a free space. For the slab of thickness d we have

$$\zeta_1 = \zeta \coth \frac{d}{\delta}, \quad \zeta_2 = \zeta / \sinh \frac{d}{\delta}, \quad \zeta = -\frac{i\omega}{c} \delta. \quad (15)$$

Transparency of this slab equals

$$T = \left| \frac{2\zeta_2}{\zeta_2^2 - (\zeta_1 - 1)^2} \right|^2. \quad (16)$$

At thickness much smaller than the penetration depth, $d \ll |\delta|$, we receive an expression

$$T \approx \left(\frac{4\pi|\delta|^2}{\lambda d} \right)^2 \quad (17)$$

where $\lambda = 2\pi c / \omega$ is the wavelength of the electromagnetic radiation in vacuum. The quality factor Q of the cavity with the bulk superconducting walls equals in terms of δ_L, δ_{sk}

$$Q = \frac{c^3}{8\delta_L^3 \sigma_2 \omega^2}. \quad (18)$$

At low temperature $T \ll \Delta$, this value is exponentially large since σ_2 becomes very small. Values of Q of order 10^{10} are readily achieved in the Nb or Nb -coated superconducting cavities [16-18].

An important issue is the dependence of the quality factor on the amplitude of RF power. The dependence is related to three basic mechanisms:

- (1) Condensate exhaustion at increasing RF amplitude;
- (2) Destruction of superconductivity in cavity walls due to nucleation of normal phase and vortex penetration;
- (3) Stray losses due to foreign inclusions and imperfections in the wall.

By the condensate exhaustion, we mean the depairing effect of large a.c. current. In case of a cavity formed by superconducting film sputtered over the surface of nonsuperconducting metal, depairing effect will decrease Δ and n_s , thus increasing the number of normal excitations and the London penetration depth. Both factors will significantly reduce the value of Q before the penetration of vortices will finally destroy superconductivity.

Destruction of superconductivity is expected to grow exponentially when a.c. component of magnetic field at the surface reaches the value of critical magnetic field. Since superconducting current in cavity is time-dependent, the supercooling and superheating critical magnetic fields will depend on frequency. The peculiarity of such dependence, as well as the relevant relaxation mechanisms responsible for superconducting state degradation remain an important issues.

In a bulk superconductor, vortex penetration starts at the lower Abrikosov critical field H_{c1} , the full destruction of superconductivity is achieved at the upper critical field H_{c2} [7].

Superconductivity near the surface of metal remains up to the field $H_{c3} = 1.69H_{c2}$ [19]. The surface layer is unstable in the parallel field, and “tilted” vortices [20] are created in the surface sheath determining RF losses and degradation mechanisms [21,22].

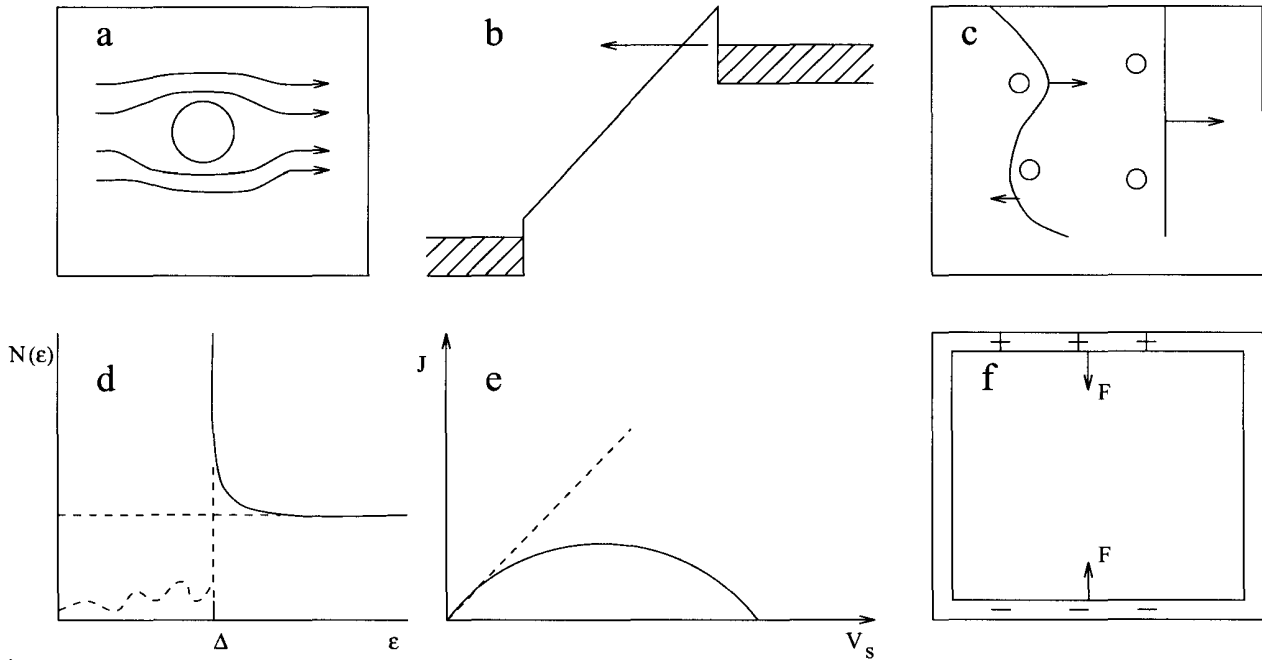


Fig.5. Phenomena near the superconducting surface related to RF losses. (a) Supercurrents bypassing a non-superconducting inclusion, (b) cold electron emission from the metal, (c) oscillation and depinning of trapped vortices, (d) quasiparticle states inside superconducting energy gap, (e) depairing mechanism, (f) deformation of the cavity wall.

Many factors influence the decrease of the cavity quality factor and its degradation at increasing RF amplitude. Among those, we mention the following.

1. Defects and surface contamination

Inclusion of non-superconducting phases, or the less- T_c phases to the cavity wall will cause the a.c. currents to choose curved path to escape penetration to normal region (Fig.5,a). The resulting increase of the current density near normal inclusion will suppress the overall critical field of the cavity. These factors may be of particular importance in the case of superconductor-coated normal-metal cavities since normal region can easily penetrate through the superconducting coating. The non-superconducting substrate becomes exposed to RF radiation which further increases losses before the bulk critical field is reached. Assuming that the low-field cavity Q value is of order 10^{10} and that the normal-state cavity $Q \approx 10^5$ we

achieve the conclusion that as small as 10^{-5} percentage of the defected surface may cause serious effect on cavity critical parameters.

2. Electron ionization

High a.c. electric field inside the cavity will depress the potential barrier for electron tunneling from metal (Fig.5,b) thus causing currents between the cavity walls. Such currents will contribute to a.c. losses and eventually destroy superconductivity at increasing RF amplitude.

3. Heating effects

Joule losses in a cavity wall heat the wall and therefore decrease the basic superconductor parameters Δ and n_s . In a *Nb*-coated cavity, the effect is expected to be less important because of much better thermal conductivity of the normal metal compared to the thermal conductivity of superconductor.

4. Trapped vortices

Abrikosov vortices can be frozen in a cavity material during its cooling down, and be pinned by defects in the wall (Fig.5,c). RF currents create a Lorentz force driving vortices out of equilibrium position. Vortex vibration at small RF amplitude, or vortex depinning at larger amplitude will lead to additional RF losses reducing cavity Q value at an increasing a.c power.

5. Quasiparticle states inside the superconducting gap

Normal-metal inclusions, point defects, linear defects like dislocations and planar defects like interphase boundaries may create quasiparticle states with energies below the gap energy of superconductor. These gapless excitations (shown schematically by the dashed line in Fig.5,d) may dominate power absorption at the concentration $n' > n_{qp}$. Since the thermal quasiparticle concentration is exponentially small at low temperature, even small amount of gapless states not easily detected in tunneling experiments may substantially alter the Q value, and thus put a limit to the cavity efficiency.

6. RF harmonic generation

At increasing RF amplitude, supercurrent vs vector-potential dependence, $j = j(A)$, becomes nonlinear (Fig.5,e), similar to the nonlinear current-phase dependence in the Josephson effect in superconducting junctions. The nonlinear current component will create odd harmonics of an a.c. electromagnetic field inside the cavity. Since harmonic components are out of resonance, they will contribute to the reflection coefficient of electromagnetic wave from the cavity wall and therefore to effective cavity losses. This effect is however practically almost negligible (except possibly at very high frequency) since the amplitude of RF current in cavity is much smaller than the depairing current of superconductor.

7. Losses in the normal substrate of *Nb* – coated cavities

T.

In the *Nb* – sputtered cavities, part of RF field penetrates to the normal substrate (typically, *Cu*). Although the amplitude of this field is much reduced due to the Meissner effect in the coating, it may compare to losses in the superconducting coating. At low temperature this contribution will dominate since quasiparticle excitation concentration in

normal metal remains finite at $T \rightarrow 0$ whereas in superconductor n_{qp} decreases exponentially at low temperature.

8. Surface conduction

Non-superconducting, and even non-metallic contamination at the surface of a cavity produces small currents under the RF field. A.c. losses due to these currents add to Joule losses in the superconducting cavity wall. Residual losses due to surface contamination may put a limit to the ultimate performance of superconducting resonators.

9. Cavity vibration and surface phonons

Among the exotic mechanisms limiting the cavity performance we mention the wall vibration which may originate from external sources like devices near the cavity, etc., and the cavity wall deformation due to mechanical forces related to large electrical fields between the opposite walls

(Fig.5,f). Smaller, but intrinsic effect may arise from the virtual surface phonons in the cavity wall.

Any displacement of the wall results in the shift of the cavity resonance frequency and therefore, at fixed input frequency, will drive system out of resonance. The effect may come to be of importance just because of very large value of Q . A wall displacement of the order of $\delta x \approx \lambda / Q$ where λ is the wavelength is of significance since it makes δx less than the atomic size at $\lambda = 10\text{cm}$ and $Q = 10^{10}$. An intrinsic effect of surface phonons corresponds to the displacement of order $\delta \bar{x} \approx (h / M \omega_D)^{1/2}$ where M is atomic mass and ω_D the Debye frequency of crystal. Only part of this displacement, of the relative magnitude ω / ω_D , contributes to the shift of cavity resonance. This gives an estimate of the maximal cavity quality factor $Q_{\text{max}} \approx \lambda \omega_D (M / h \omega)^{1/2}$. In table 2, we summarize the ranges of cavity frequencies and Q factors for which the above discussed effects of mechanical forces (MF) and surface phonons (SF) may be of importance.

Table 2

Effect of mechanical force and surface phonons on superconducting cavities

$Q / f, \text{Hz}$	10^8	10^9	10^{10}
10^{10}			SP
10^{12}	MF	SP	SP
10^{14}	MF, SP	MF, SP	SP

In conclusion, many extrinsic factors can influence the ultimate performance of high-frequency, high-power applications of superconductivity. Intrinsic mechanisms of RF losses in superconducting cavities which are widely used in particle accelerators including the condensate exhaustion (the depairing effect of an a.c. current) and superconductivity

nucleation mechanisms related in particular to surface superconductivity and “tilted” vortices require better theoretical understanding.

References

1. J. de Nobel and P.Lindenfeld. *Phys. Today* **49**, N0.9, 40 (1996).
2. H.Kamerlingh Onnes. *Leiden Commun.* **120b**, **122b**, **124c** (1911).
3. G.Bednorz and K.A.Mueller. *Zs. Phys.* **B64**, 189 (1986).
4. M.K.Wu, J.R.Ashburn, C.W.Chu et al. *Phys. Rev. Lett.* **58**, 908 (1987).
5. J.Bardeen, L.N.Cooper and J.R.Schrieffer. *Phys. Rev.* **108**, 1175 (1957).
6. V.L.Ginzburg and L.D.Landau. *Zh. Eksp. Teor. Fiz.* **20**, 1064 (1950).
7. A.A.Abrikosov. *Sov. Phys. JETP* **5**, 1174 (1957).
8. L.P.Gorkov. *Sov. Phys. JETP* **9**, 1364 (1959).
9. A.A.Abrikosov. *Fundamentals of the Theory of Metals*. North-Holland, Amsterdam, 1998.
10. I.O.Kulik. *JETP Lett.* **11**, 275 (1970).
11. M.Buttiker, J.Imry and R.Landauer. *Phys. Lett.* **A96**, 365 (1983).
12. M.Tinkham. *Introduction to Superconductivity*, 2nd edition. McGraw-Hill, Inc, 1996.
13. A.A.Abrikosov, L.P.Gorkov and I.M.Khalatnikov. *Sov. Phys. JETP* **8**, 182 (1959).
14. D.C.Mattis and J.Bardeen. *Phys. Rev.* **111**, 412 (1958).
15. I.O.Kulik. *Sov. Phys. JETP* **28**, 461 (1969).
16. G.Fortuna, R.Pengo, A.Lombardi et al. *Proc. Europ. Particle Accelerator Conf.*, vol.1, p.43. Eds. P.Martin and P.Mandrillon, 1990.
17. I.Ben-Zvi, E.Chiavery, B.V.Elkonen et al., *ibid.*, p.1103.
18. V.Palmieri, V.L.Ruzinov. S.Yu.Stark et al. *Nucl. Instr. and Methods in Phys. Res.* **A328**, 280 (1993).
19. D.Saint-James and P.G. de Gennes. *Phys Lett.* **7**, 306 (1963).
20. I.O.Kulik. *Sov. Phys. JETP* **30**, 329 (1969).
21. K.Maki. *J. Low Temp. Phys.* **4**, 545 (1970).
22. Y.Brunet, P.Monceau and G.Waysand. *Phys. Rev.* **5**, 1927 (1974).